Supplement of Atmos. Chem. Phys., 24, 9475–9514, 2024
https://doi.org/10.5194/acp-24-9475-2024-supplement

Atmospheric Chemistry and Physics
Open Access
EGU

Supplement of

Technical note: Evaluation of the Copernicus Atmosphere Monitoring Service Cy48R1 upgrade of June 2023

Henk Eskes et al.

Correspondence to: Henk Eskes (henk.eskes@knmi.nl)

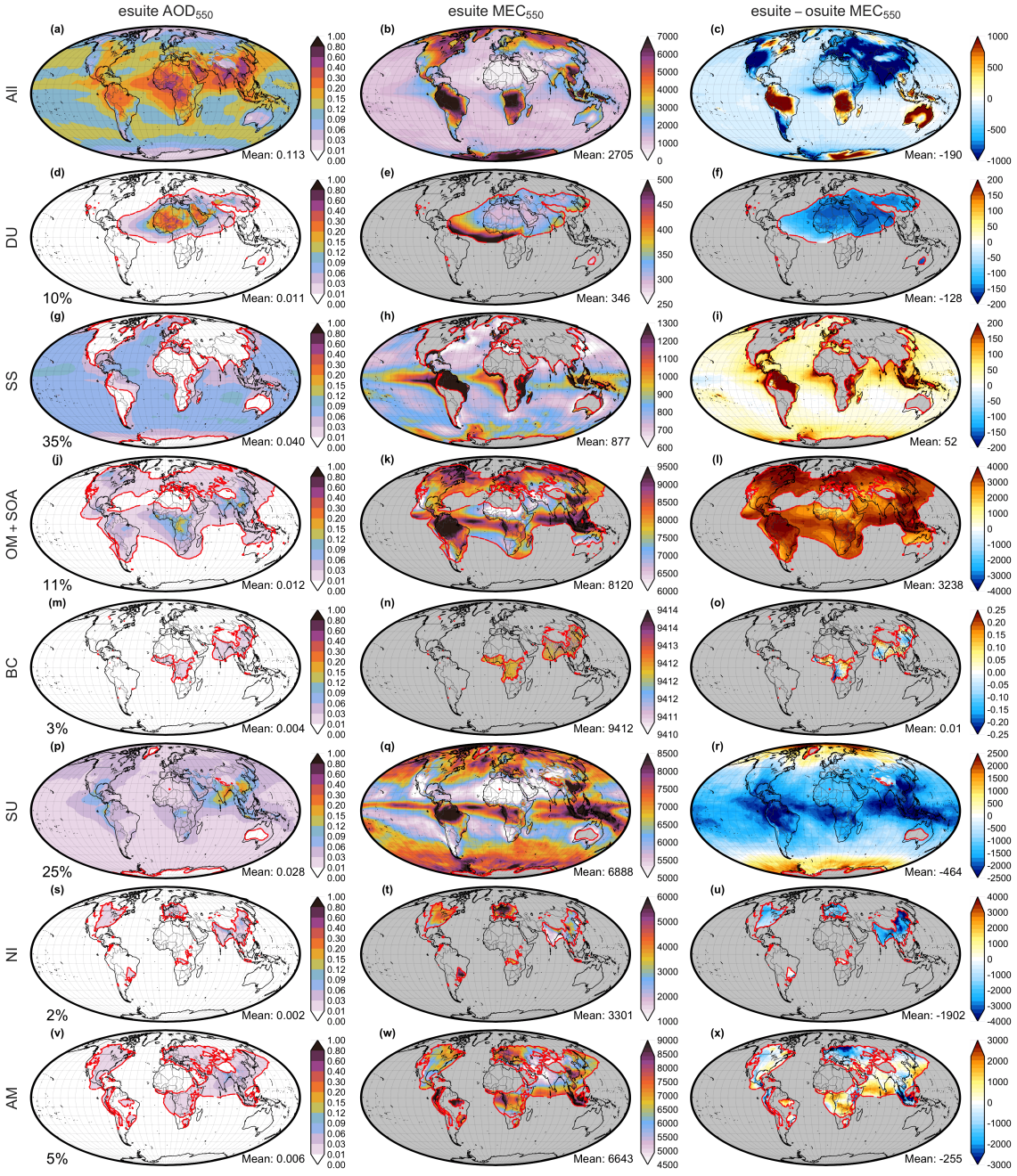

Figure S 1. The aerosol optical depth at 550nm (1st column), mass extinction coefficient, calculated as the ratio of aerosol optical depth to aerosol mass (2^{nd} row) and the mass extinction coefficient difference between e-suite minus o-suite for the period 2022-10-01 to 2023-06-27. Mass extinction coefficient and mass extinction difference between e-suite and o-suite is only depicted for aerosol optical depth higher than 0.01 for the aerosol species (red outline). Percentage at the bottom right corner of 1st column displays the relative contribution of each species optical depth to AOD.

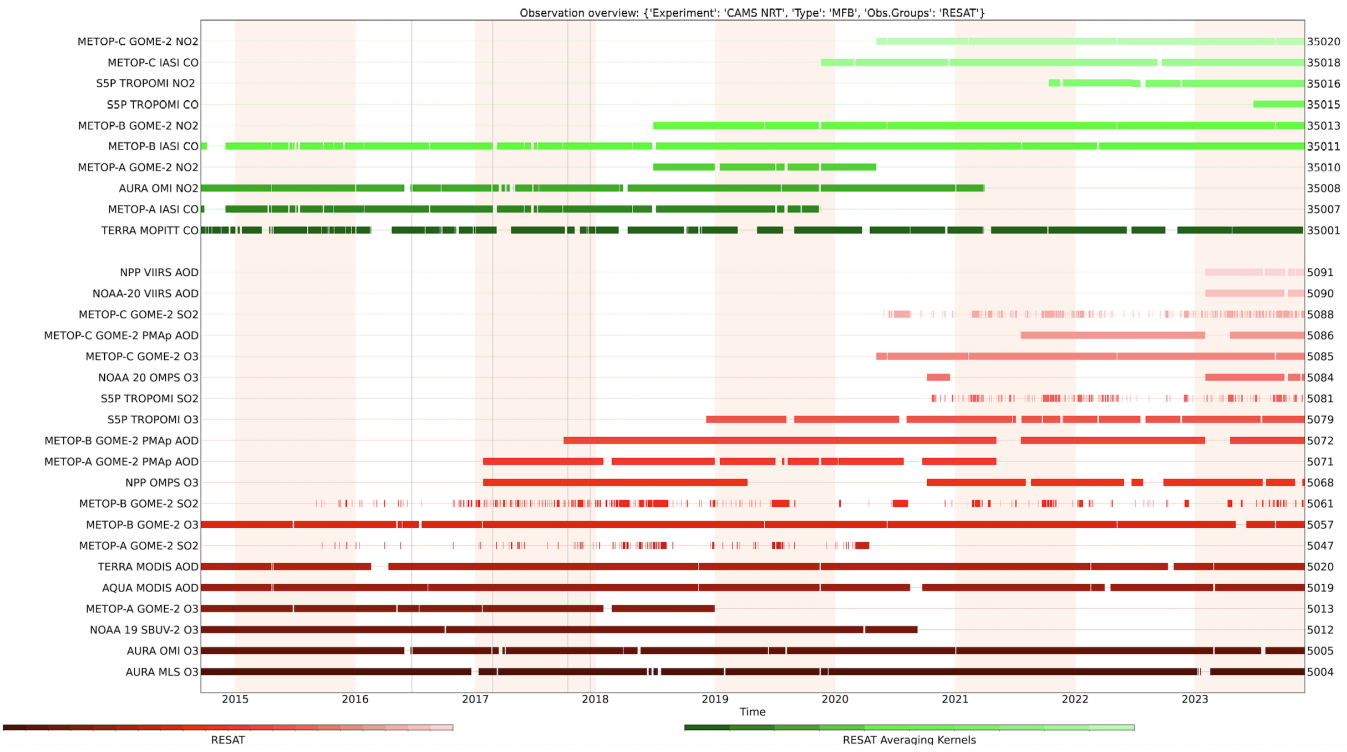

Figure S 2. Satellite observation usage in the o-suite, for ozone, CO, aerosol AOD, SO_2 and NO_2, from October 2014 until 1 December 2023. Note that this includes Cy48R1 from the date it became operational, 27 June 2023. Top rows (in green): products assimilated using averaging kernels; bottom rows (in red): without averaging kernels. The most recent additions in the assimilation system are the AOD from VIIRS (NPP & NOAA-20) and CO from TROPOMI (Sentinel-5P).

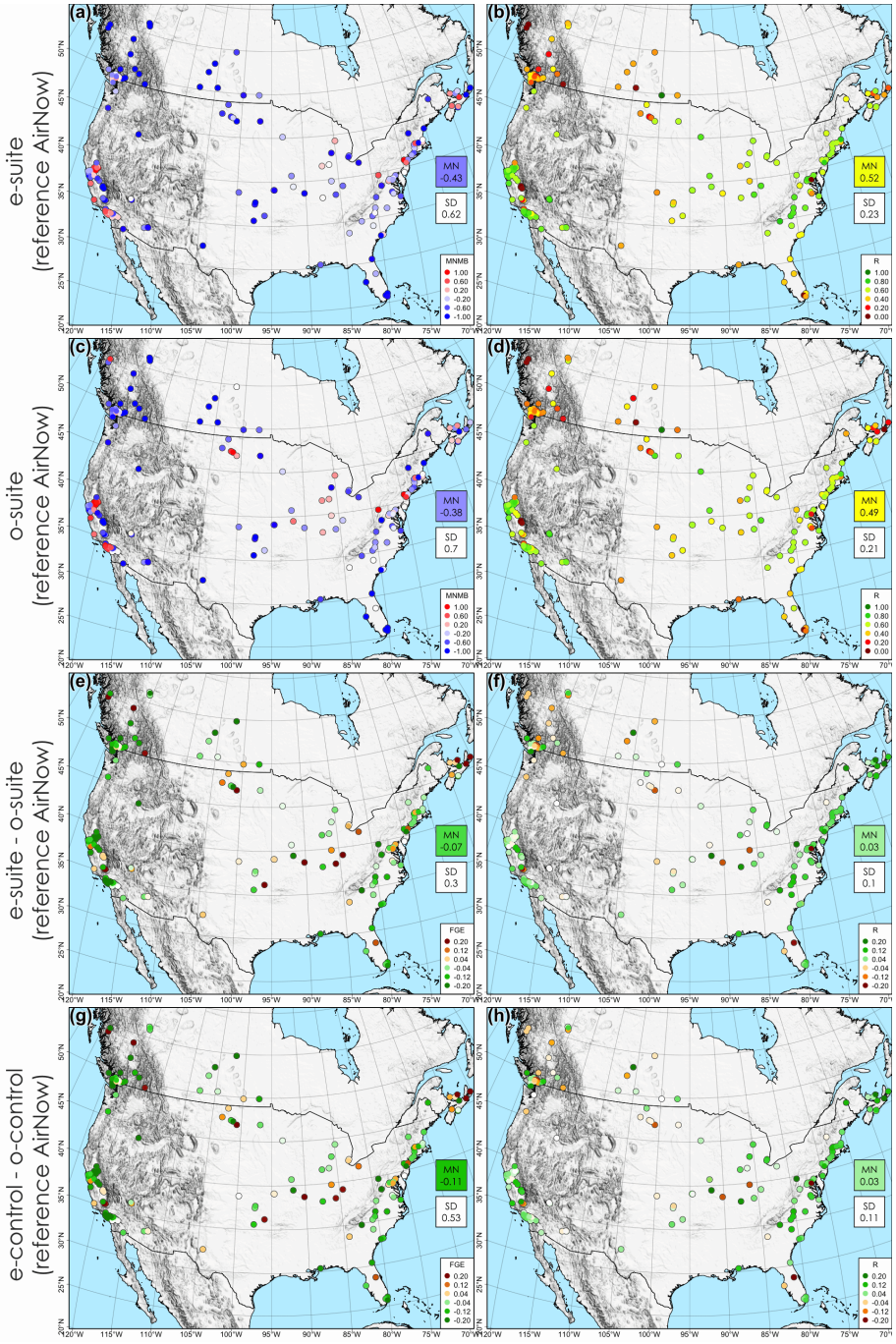

Figure S 3. Spatial distribution of the daily NO_2 evaluation over the USA and Canada, for the e-suite minus AirNow observations (first row, left: MNMB, right: R), the o-suite minus observations (second row, left: MNMB, right: R), the e-suite minus the o-suite differences (third row, left: FGE, right: R) and the e-control minus the o-control differences (fourth row, left: FGE, right: R) for the period 2023-10-01 to 2023-06-27. The mean (MN) and standard deviation (SD) for all station is depicted for each map.

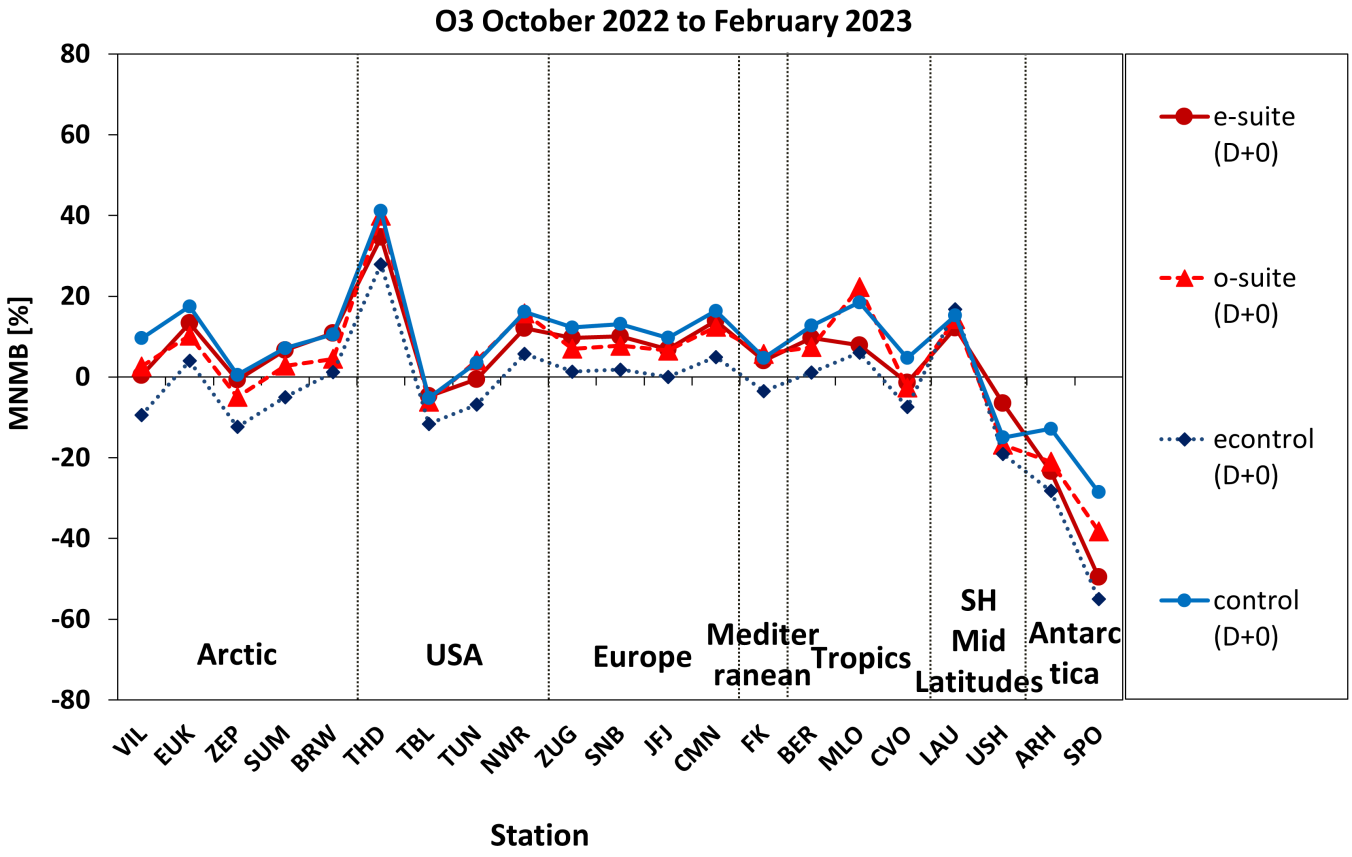

Figure S 4. Ozone modified normalised mean bias for the e-suite (red, solid), o-suite (red dashed) and corresponding control runs (blue) using as a reference WMO-GAW, ESRL/GMD and Arctic IASOA surface stations during the period 1 October 2022 to 28 February 2023.

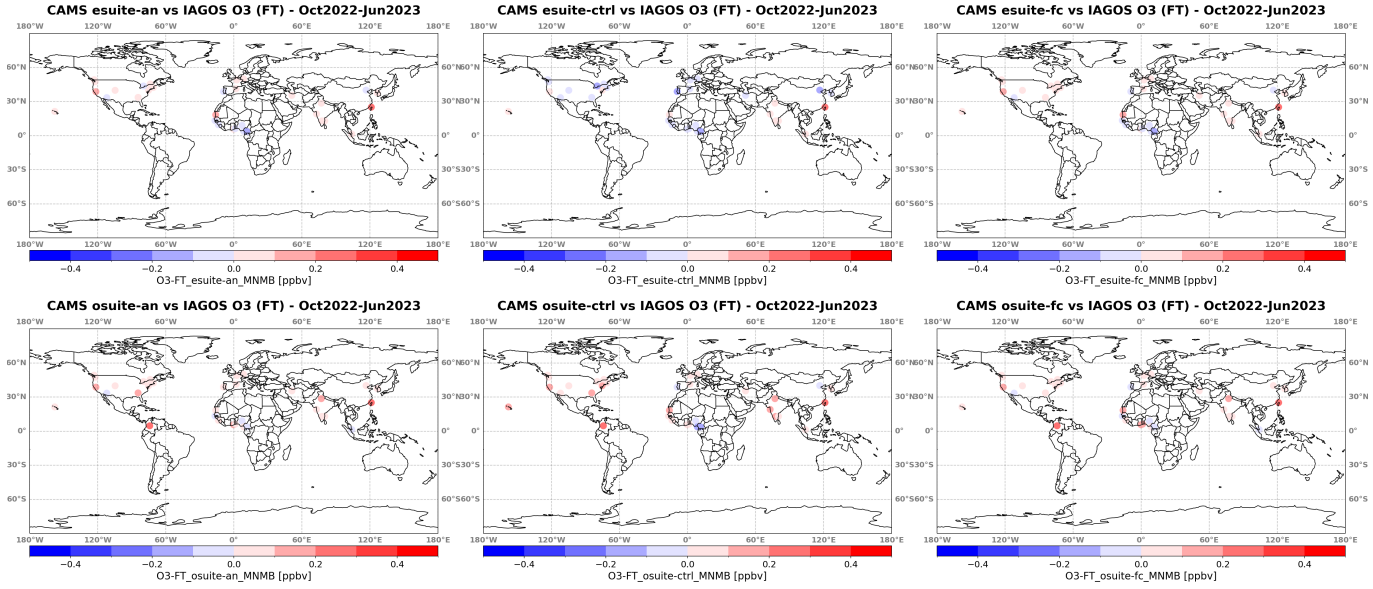

Figure S 5. Ozone comparisons using aircraft profile observations from IAGOS (http://www.iagos.org). Map of CAMS IAGOS MNMB from the e-suite on the top row (left: analysis, middle: control run: right: 1-day forecast) and o-suite on the bottom row for ozone in the free troposphere (FT) based on profile observations at the different airports visited during the period October 2022 – June 2023.

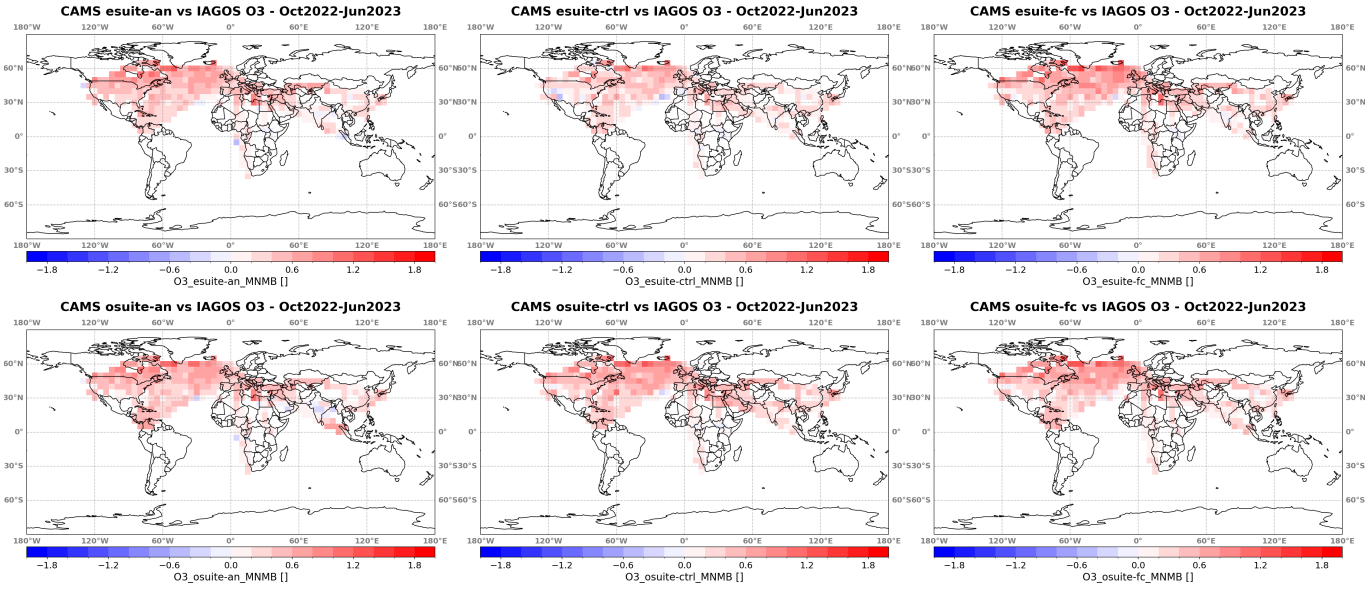

Figure S 6. Ozone comparisons using aircraft observations from IAGOS (http://www.iagos.org). Global maps of CAMS IAGOS MNMB (gridded to 5x5 degrees) from the e-suite (top panels, from left to right : analysis, control run and 1-day forecast) and o-suite (bottom panels, from left to right: analysis, control run and 1-day forecast) for ozone in the Upper Troposphere (UT) based on IAGOS-cruise data (filtered observations with PV values below 2) during the period October 2022 - June 2023.

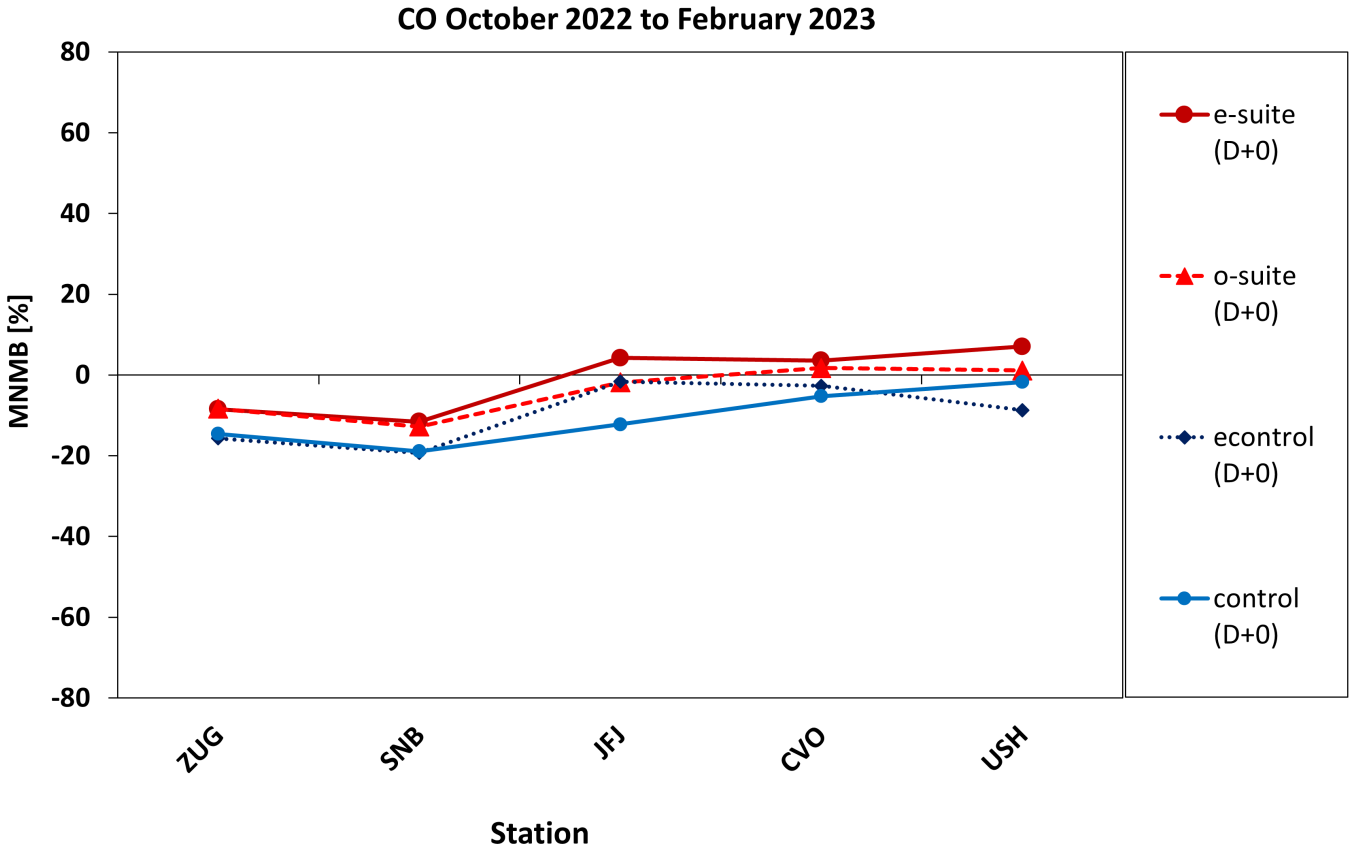

Figure S 7. Carbon Monoxide comparisons using WMO-GAW surface observations for the period 1 October 2022 to 28 February 2028. The plots show the modified normalised mean bias for the e-suite (red, solid), o-suite (red dashed) and corresponding control runs (blue). Biases are small and are similar for the e-suite and o-suite.

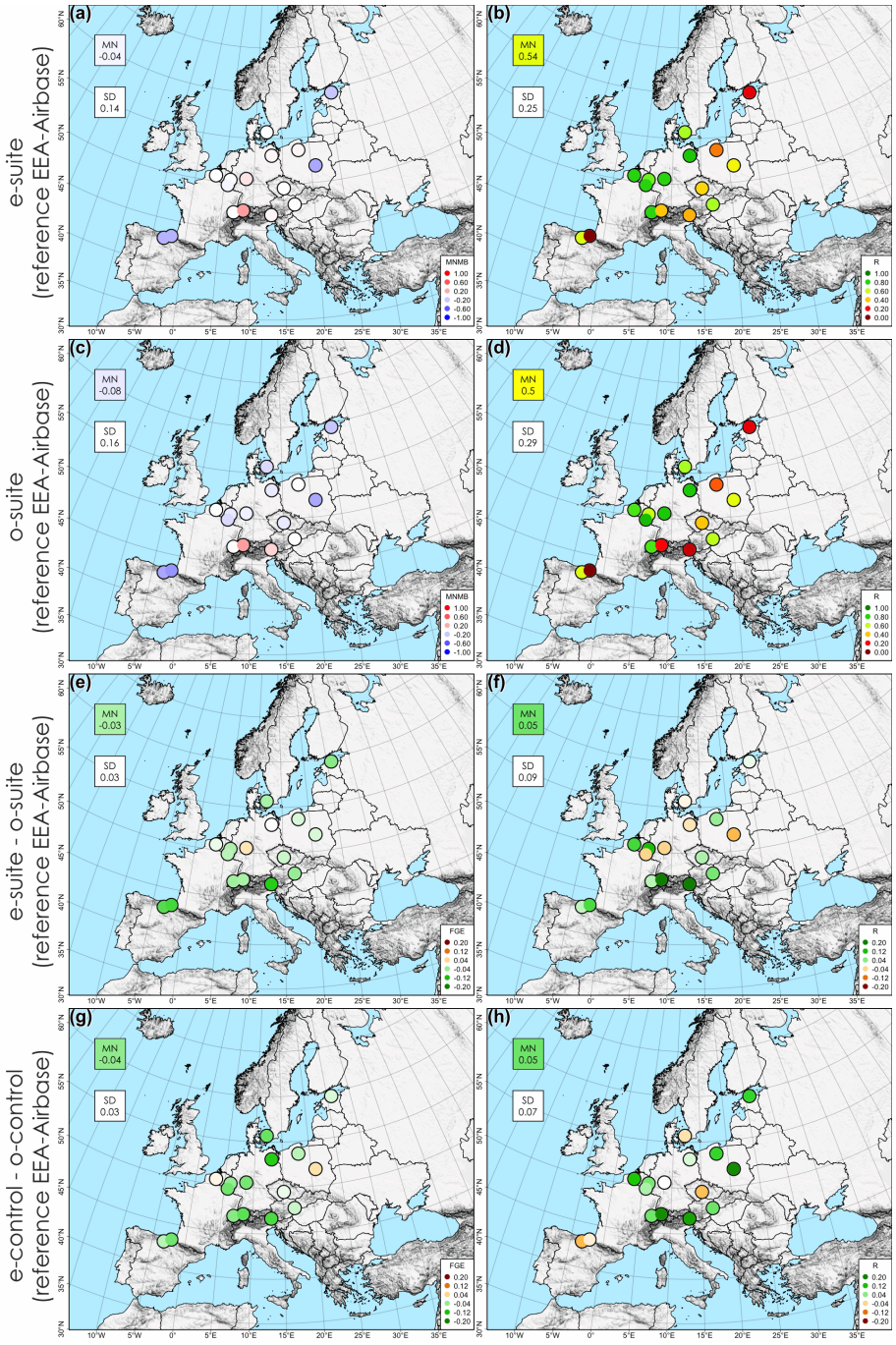

Figure S 8. Spatial distribution of the daily CO evaluation over Europe, for the e-suite minus EEA-Airbase observations (first row, left: MNMB, right: R), the o-suite minus observations (second row, left: MNMB, right: R), the e-suite minus the o-suite differences (third row, left: FGE, right: R) and the e-control minus the o-control differences (fourth row, left: FGE, right: R) for the period 2023-10-01 to 2023-06-27. The mean (MN) and standard deviation (SD) for all station is depicted for each map.

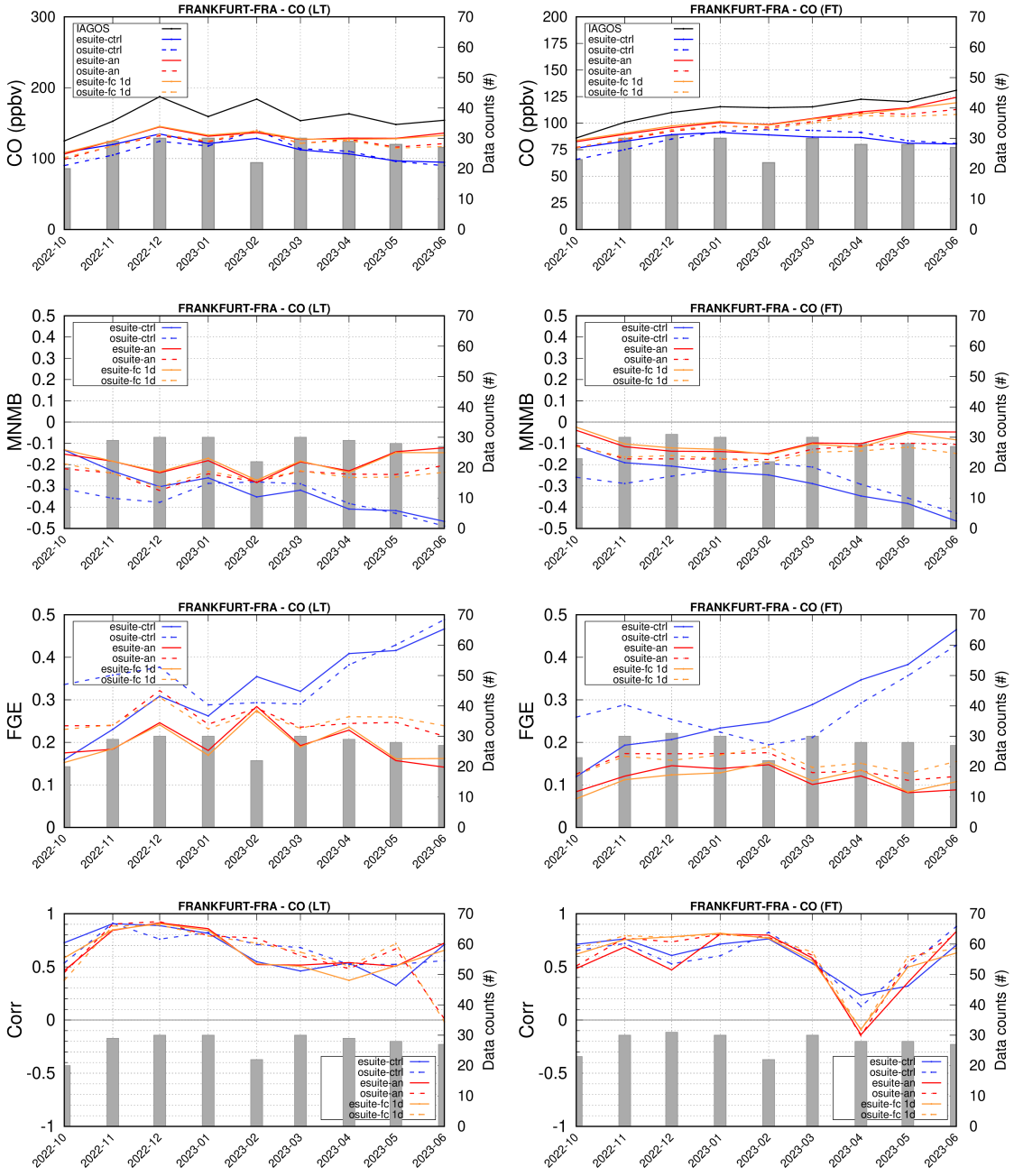

Figure S 9. CO comparisons using aircraft observations from IAGOS (http://www.iagos.org). Monthly time series for CO from IAGOS aircraft observations, from e-suite (solid) and the o-suite (dashed) for analysis (red), 1-day forecast (orange) and control run (blue) as well as associated scores CAMS-IAGOS (top: MNMB, middle: FGE, bottom: Pearson Correlation) at Frankfurt in two different atmospheric layers (left: Low Troposphere LT, right: Free Troposphere FT) during the period October 2022 - June 2023. The histogram bars indicate the number of profiles (i.e. layer values) based on available observations.

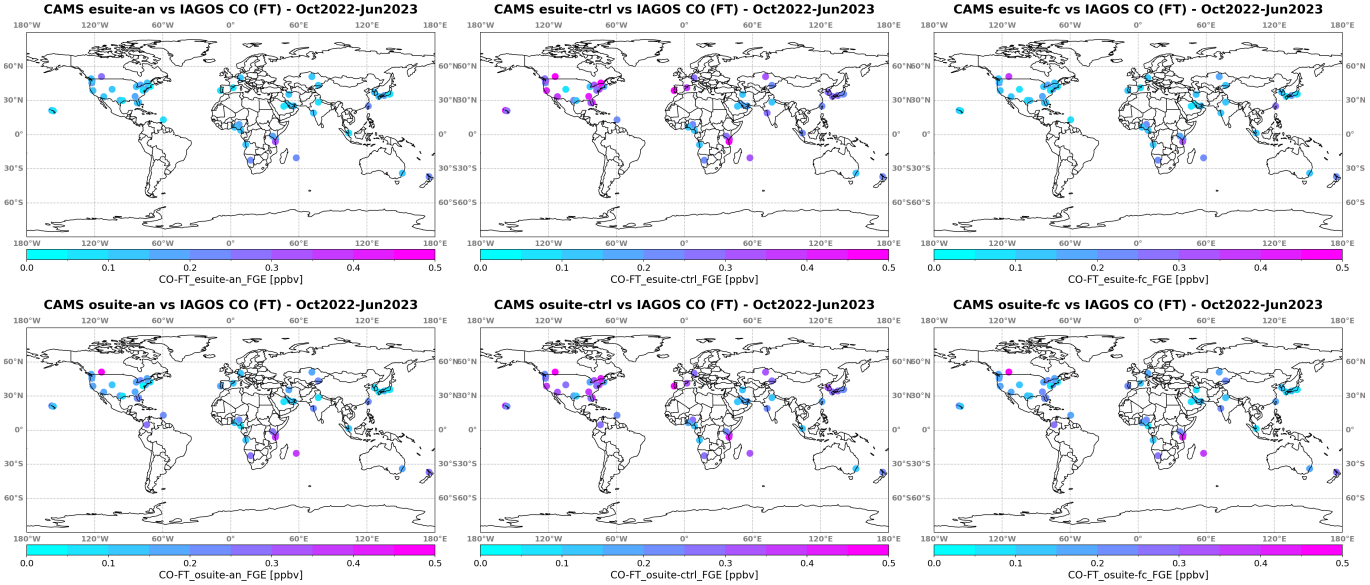

Figure S 10. CO comparisons using aircraft observations from IAGOS (http://www.iagos.org). Map of CAMS-IAGOS FGE from the e-suite on the top row (left: analysis, middle: control run, right: 1-day forecast) and o-suite on the bottom row for CO in the free troposphere (FT) based on profile observations at the different airports visited during the period October 2022 – June 2023.

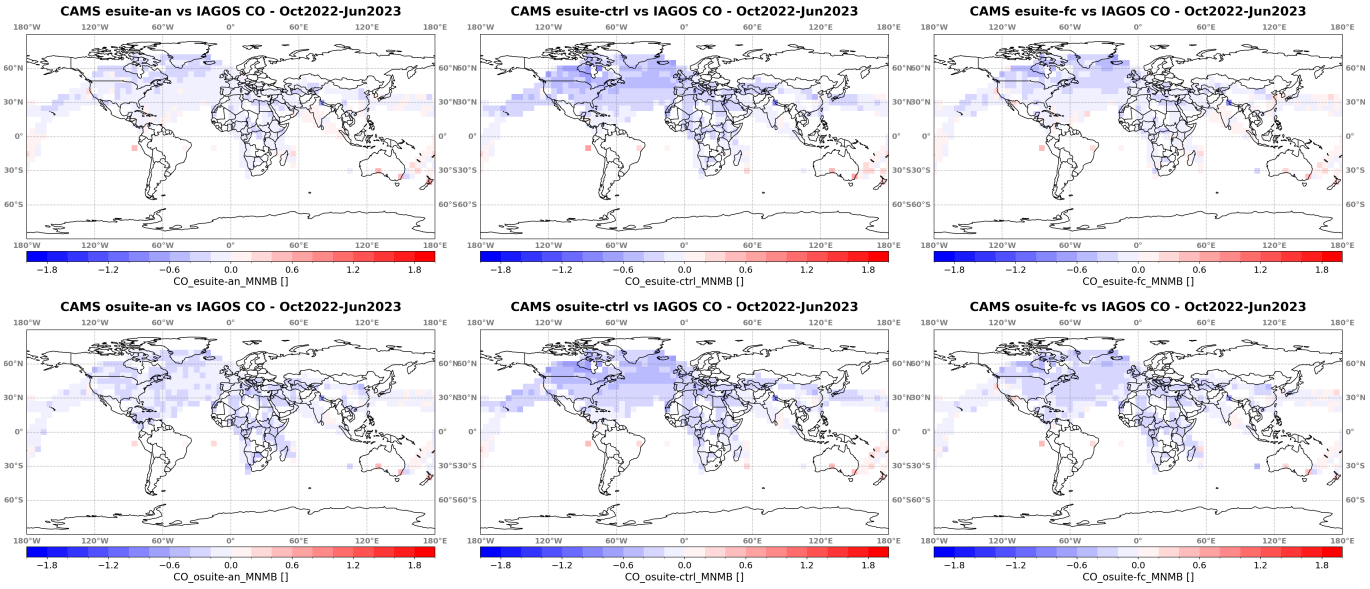

Figure S 11. Global maps of CAMS-IAGOS MNMB (gridded to 5x5 degrees) from the e-suite (top panels, from left to right : analysis, control run and 1-day forecast) and o-suite (bottom panels, from left to right : analysis, control run and 1-day forecast) for CO in the Upper Troposphere (UT) based on IAGOS-cruise data (filtered observations with PV values below 2) during the period October 2022 - June 2023.

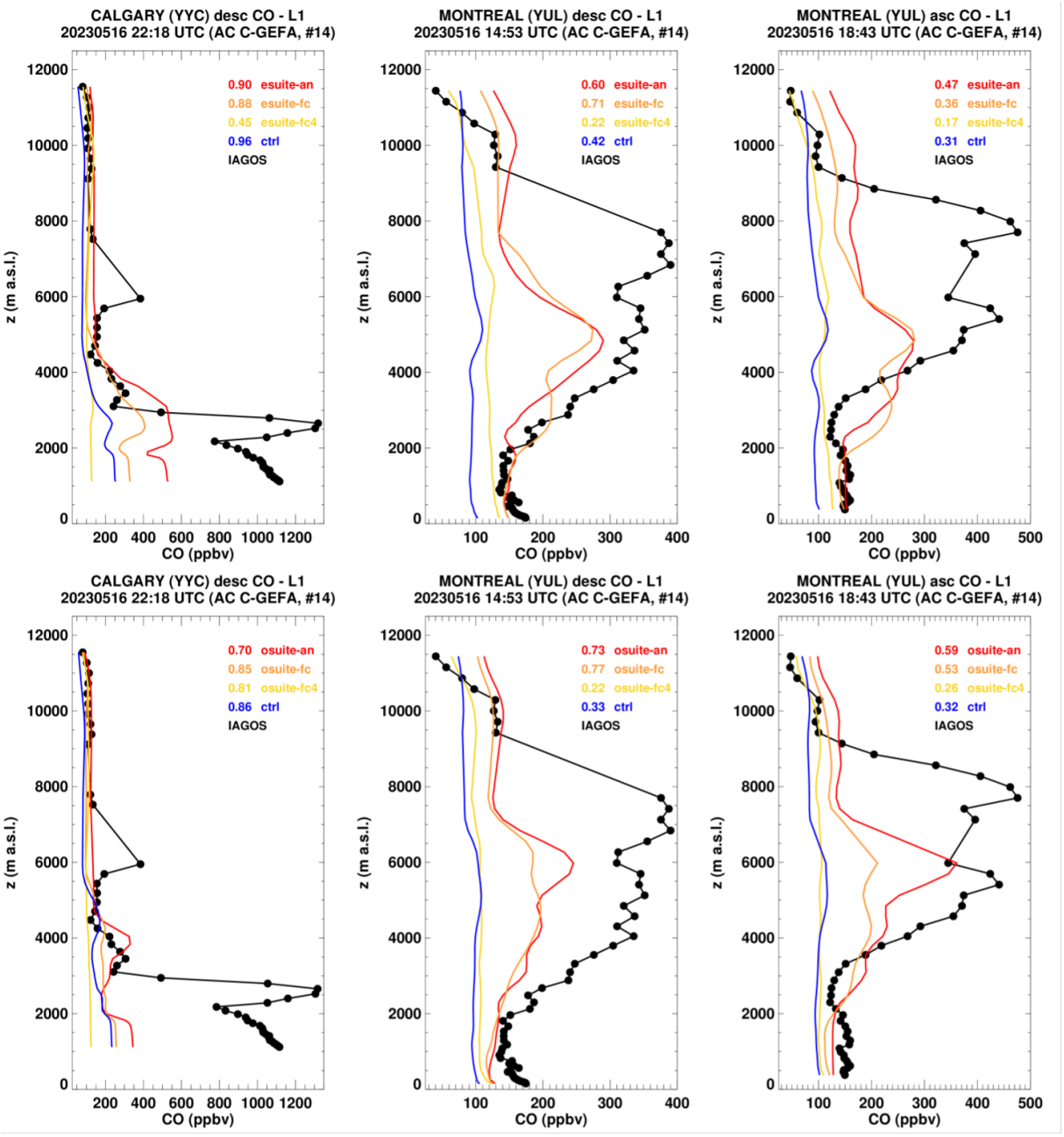

Figure S 12. Selection of IAGOS aircraft CO profiles from May 2023 at Montreal and Calgary airports sampled by aircraft operated by Air Canada, showing the transport of plumes from forest wildfires occurring in the Canadian province of Alberta. IAGOS observations are shown in black, and colored curves show the CAMS modeled profiles from the e-suite (top panels) and the o-suite (bottom panels) analysis (red), 1-day forecast (orange), 4-day forecast yellow and e-suite and o-suite control run (blue). Units (ppbv).

Table S 1. Overview statistics for tropospheric CO column differences at 13 NDACC FTIR stations (rows). Statistics are shown for the e-suite (left) and o-suite (right) analysis and controls for the period October 2022 to February 2023. Shown are the number of matched observations (count), the ratio of the standard deviation in the tropospheric columns for the o/e-suite and the FTIR time series (ratio std), the Pearson correlation coefficient, the normalised mean bias (NMB) and standard deviation of the bias (std NMB). The bias for the e-suite is reduced for almost all sites. Although correlations are similar for the o-suite and e-suite, the ratio of the standard deviation in the tropospheric columns for the e-suite and the FTIR time series is higher compared to the o-suite. For the tropical sites the bias has switched sign and is now positive.

		e-suiteAN					**o-suiteAN**				
FTIR	latitude [degrees-north]	count	ratio std [1]	Pearson [1]	mean NMB [%]	std NMB [%]	count	ratio std [1]	Pearson [1]	mean NMB [%]	std NMB [%]
THULE	76.52	39	0.92	0.89***	−18.54	3.45	39	0.95	0.86***	−17.16	3.52
ST.PETERSBURG	59.88	24	1.32	0.92***	−4.71	4.75	24	1.05	0.95***	−2.94	3.61
BREMEN	53.10	8	1.29	0.73**	−5.59	5.29	8	0.90	0.75**	−9.36	5.53
ZUGSPITZE	47.42	70	0.76	0.72***	−4.22	5.75	70	0.71	0.75***	−12.37	5.91
JUNGFRAUJOCH	46.55	11	1.06	0.76***	−11.39	6.47	11	0.73	0.60*	−16.41	7.68
TORONTO.TAO	43.60	125	0.85	0.90***	−6.58	5.59	125	0.91	0.90***	−8.28	5.02
BOULDER.CO	40.04	155	0.97	0.90***	−10.66	6.10	155	1.03	0.92***	−14.31	5.44
MAUNA.LOA.HI	19.54	34	0.86	0.98***	6.63	2.62	34	0.86	0.97***	−11.23	3.68
PARAMARIBO	5.81	2	0.59	1.00	2.90	5.43	2	0.53	1.00	−7.11	5.84
LA.REUNION.MAIDO	−21.08	22	0.99	0.97***	9.67	3.65	22	0.93	0.97***	−4.95	4.55
WOLLONGONG	−34.41	165	0.94	0.81***	0.99	9.66	165	0.98	0.79***	−11.38	9.14
LAUDER	−45.04	149	0.99	0.96***	0.48	5.24	149	0.97	0.98***	−8.33	4.14
ARRIVAL.HEIGHTS	−77.82	61	0.91	0.98***	6.38	5.22	61	1.10	0.98***	6.20	4.62
mean		66	0.96	0.87	−2.67	5.32	66	0.90	0.87	−9.05	5.28
		e-control					**control**				
FTIR	latitude [degrees-north]	count	ratio std [1]	Pearson [1]	mean NMB [%]	std NMB [%]	count	ratio std [1]	Pearson [1]	mean NMB [%]	std NMB [%]
THULE	76.52	25	1.30	0.83***	−24.03	1.29	36	0.97	0.99***	−19.95	4.10
ST.PETERSBURG	59.88	24	1.59	0.82***	−13.92	6.54	24	0.85	0.92***	−12.92	6.66
BREMEN	53.10	7	0.80	0.68*	−12.50	5.21	7	0.50	0.75**	−16.42	8.45
ZUGSPITZE	47.42	70	1.27	0.87***	−7.55	2.88	70	0.95	0.82***	−14.58	3.76
JUNGFRAUJOCH	46.55	11	1.08	0.55*	−10.76	6.00	11	0.86	0.86***	−10.17	3.82
TORONTO.TAO	43.60	95	1.02	0.70***	−12.72	6.31	95	0.76	0.74***	−13.88	7.76
BOULDER.CO	40.04	142	1.09	0.64***	−7.32	8.28	145	0.89	0.79***	−10.01	7.56
MAUNA.LOA.HI	19.54	34	0.83	0.97***	−3.99	3.50	35	1.01	0.93***	−8.23	3.65
PARAMARIBO	5.81	2	0.83	1.00	−17.44	3.13	2	0.85	1.00	−22.86	3.32
LA.REUNION.MAIDO	−21.08	22	2.33	0.73***	−7.09	9.66	22	1.90	0.63***	−11.59	9.79
WOLLONGONG	−34.41	156	0.94	0.66***	1.22	11.98	158	1.13	0.71***	−1.10	10.33
LAUDER	−45.04	143	1.22	0.87***	2.03	8.16	149	1.30	0.91***	1.65	6.83
ARRIVAL.HEIGHTS	−77.82	61	1.18	0.99***	−5.81	3.64	62	1.17	0.99***	−1.51	3.68
mean		60	1.19	0.78	−9.22	5.89	62	1.01	0.84	−10.89	6.13

Table S 2. Overview statistics for stratospheric CO column differences at 13 NDACC FTIR stations (rows). Statistics are shown for the e-suite (left) and o-suite (right) analysis and controls for the period October 2022 to February 2023. Shown are the number of matched observations (count), the ratio of the standard deviation in the tropospheric columns for the o/e-suite and the FTIR time series (ratio std), the Pearson correlation coefficient, the normalised mean bias (NMB) and standard deviation of the bias (std NMB). The bias for the e-suite is reduced significantly for the southern hemispheric sites and is now of the order of the measurement uncertainty. The SH correlations are also higher (in particular for the Antarctic site Arrival Heights). In the northern hemisphere the e-suite and o-suite perform similar.

		e-suiteAN					**o-suiteAN**				
FTIR	latitude [degrees-north]	count	ratio std [1]	Pearson [1]	mean NMB [%]	std NMB [%]	count	ratio std [1]	Pearson [1]	mean NMB [%]	std NMB [%]
THULE	76.52	39	0.90	0.74***	−26.55	11.11	39	0.79	0.78***	−25.02	11.73
ST.PETERSBURG	59.88	24	1.59	0.34	−15.93	26.56	24	1.57	0.23	−18.11	28.20
BREMEN	53.10	8	0.96	0.98***	−6.57	8.55	8	0.80	0.98***	−6.82	12.42
ZUGSPITZE	47.42	70	1.12	0.93***	3.08	10.56	70	1.03	0.94***	0.34	9.75
JUNGFRAUJOCH	46.55	11	0.86	0.97***	−3.93	9.42	11	0.77	0.94***	−7.56	12.11
TORONTO.TAO	43.60	125	0.88	0.96***	7.95	9.83	125	0.83	0.97***	5.09	10.79
BOULDER.CO	40.04	155	1.05	0.86***	−7.35	12.88	155	1.11	0.84***	−14.10	12.77
MAUNA.LOA.HI	19.54	34	0.77	0.99***	18.98	8.24	34	0.85	0.97***	−7.56	11.45
PARAMARIBO	5.81	2	1.43	1.00	3.88	5.78	2	0.59	1.00	17.54	17.19
LA.REUNION.MAIDO	−21.08	22	0.79	0.99***	12.18	6.63	22	0.95	0.99***	12.14	9.82
WOLLONGONG	−34.41	165	0.95	0.98***	4.90	9.14	165	0.98	0.94***	5.10	15.38
LAUDER	−45.04	149	0.95	0.92***	12.10	10.66	149	0.82	0.86***	20.05	17.36
ARRIVAL.HEIGHTS	−77.82	61	0.80	0.91***	17.34	12.74	61	0.40	0.55***	27.06	40.46
mean		66	1.00	0.93	1.54	10.93	66	0.88	0.89	0.63	16.11
		e-control					**control**				
FTIR	latitude [degrees-north]	count	ratio std [1]	Pearson [1]	mean NMB [%]	std NMB [%]	count	ratio std [1]	Pearson [1]	mean NMB [%]	std NMB [%]
THULE	76.52	25	1.01	0.50**	−20.57	9.38	36	1.19	0.40**	−26.09	11.96
ST.PETERSBURG	59.88	24	1.51	0.67***	−16.49	18.49	24	1.50	0.56***	−31.13	18.12
BREMEN	53.10	7	0.99	0.98***	−8.75	6.81	7	1.11	0.97***	−16.35	6.94
ZUGSPITZE	47.42	70	1.10	0.95***	0.14	8.27	70	1.05	0.91***	−10.73	8.95
JUNGFRAUJOCH	46.55	11	0.83	0.96***	−2.46	8.01	11	0.89	0.97***	−11.56	6.87
TORONTO.TAO	43.60	95	0.90	0.98***	5.55	7.60	95	0.93	0.98***	−1.79	7.38
BOULDER.CO	40.04	142	0.95	0.95***	−0.18	9.13	145	1.07	0.93***	−15.85	9.56
MAUNA.LOA.HI	19.54	34	0.77	0.95***	16.31	8.87	35	0.89	0.94***	−0.84	12.49
PARAMARIBO	5.81	2	1.39	1.00	−1.44	5.20	2	1.67	1.00	−9.28	5.72
LA.REUNION.MAIDO	−21.08	22	0.93	1.00***	5.99	7.83	22	1.08	0.99***	−0.04	6.30
WOLLONGONG	−34.41	156	0.89	0.97***	13.96	9.85	158	0.94	0.97***	4.88	9.30
LAUDER	−45.04	143	0.99	0.90***	26.00	13.17	149	0.95	0.89***	11.30	11.29
ARRIVAL.HEIGHTS	−77.82	61	0.68	0.83***	14.95	18.93	62	0.62	0.69***	−8.08	25.60
mean		60	1.00	0.89	2.54	10.12	62	1.07	0.85	−8.89	10.81

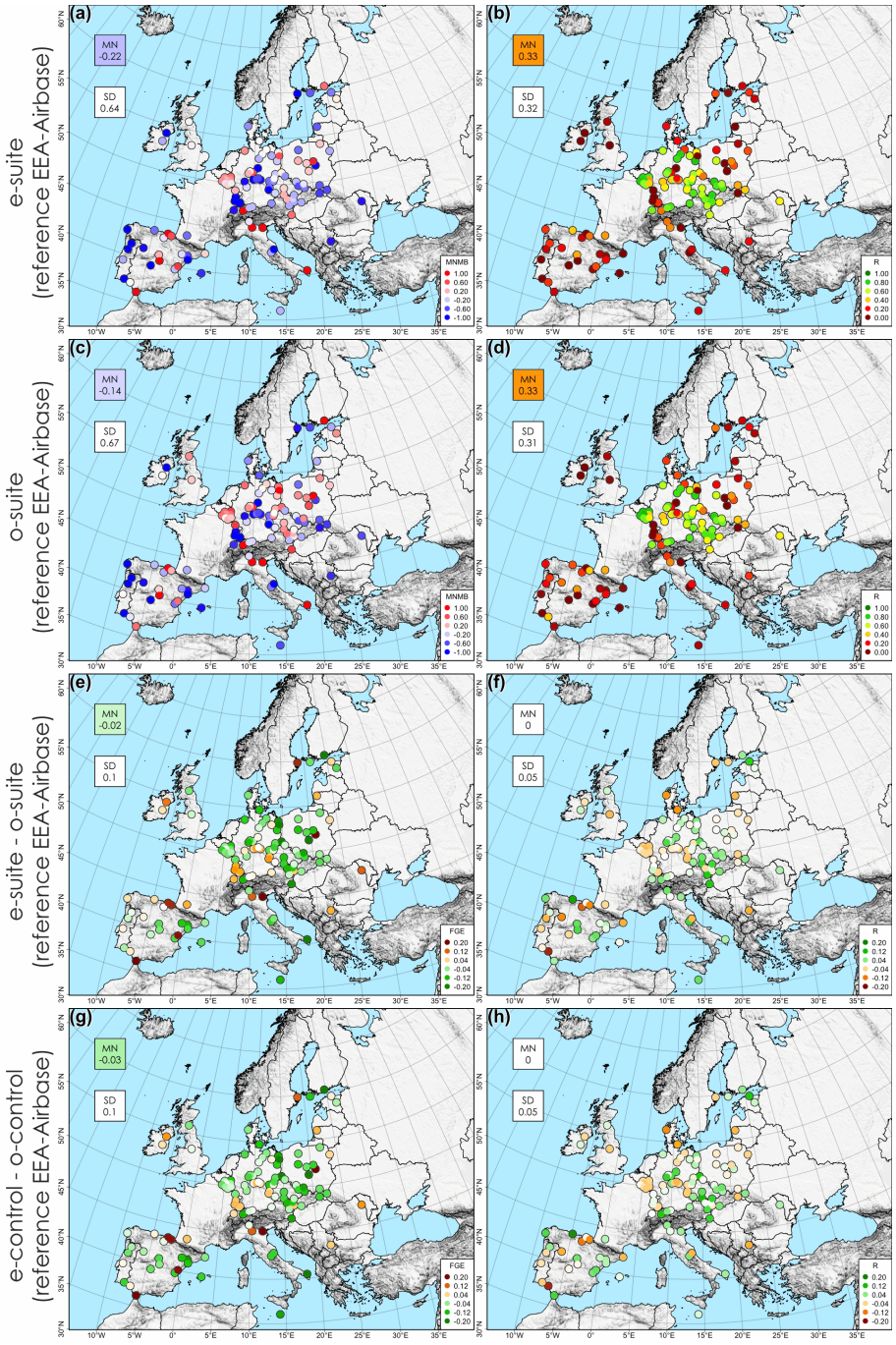

Figure S 13. Spatial distribution of the daily NO2 evaluation over Europe, for the e-suite minus EEA-Airbase observations (first row, left: MNMB, right: R), the o-suite minus observations (second row, left: MNMB, right: R), the e-suite minus the o-suite differences (third row, left: FGE, right: R) and the e-control minus the o-control differences (fourth row, left: FGE, right: R) for the period 2023-10-01 to 2023-06-27. The mean (MN) and standard deviation (SD) for all station is depicted for each map.

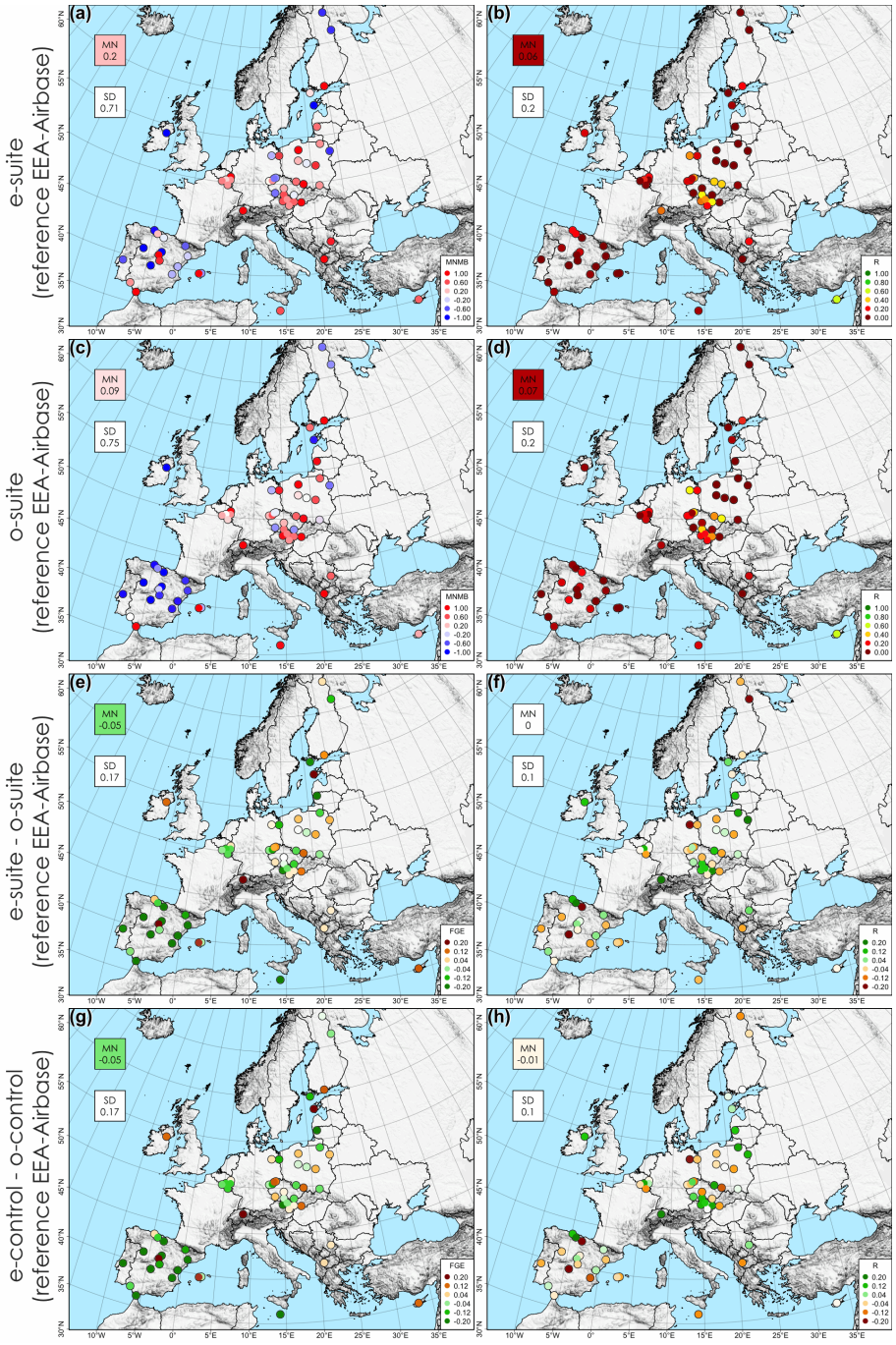

Figure S 14. Spatial distribution of the daily SO2 evaluation over Europe, for the e-suite minus EEA-Airbase observations (first row, left: MNMB, right: R), the o-suite minus observations (second row, left: MNMB, right: R), the e-suite minus the o-suite differences (third row, left: FGE, right: R) and the e-control minus the o-control differences (fourth row, left: FGE, right: R) for the period 2023-10-01 to 2023-06-27. The mean (MN) and standard deviation (SD) for all station is depicted for each map.